

## Research Article

# A Genetically Encoded Multifunctional TRAIL Trimer Facilitates Cell-Specific Targeting and Tumor Cell Killing

Dirk Spitzer<sup>1</sup>, Jonathan E. McDunn<sup>2</sup>, Stacey Plambeck-Suess<sup>1</sup>, Peter S. Goedegebuure<sup>1</sup>, Richard S. Hotchkiss<sup>2</sup>, and William G. Hawkins<sup>1</sup>

## Abstract

Tumor necrosis factor–related apoptosis-inducing ligand (TRAIL, Apo2L) has been shown to exhibit potent and specific apoptotic activity against tumor cells. Several TRAIL constructs have been tried in patients, and the molecule remains under active clinical investigation. Native and recombinant TRAIL must form a homotrimer to become biologically active. However, noncovalently associated TRAIL displays a high degree of sensitivity to degradation, which limits its therapeutic potential. To enforce trimerization of the recombinant protein, we developed a covalently linked TRAIL trimer (TR3) by genetic fusion. This molecular drug design conferred improved stability without altering the native killing ability of TRAIL. Target specificity was shown by blocking TR3 activity with soluble death receptor 5 (DR5-Fc). In addition, we have shown that TR3 is amenable to further, genetic modifications. The incorporation of additional functional domains to TR3, such as antibody fragments (scFvs) that allow for a more cell-specific delivery of the agent, is stoichiometrically controlled and inconsequential with regard to the bioactivity of TRAIL. As proof of this concept, TR3 activity was targeted to the mouse RBC membrane. TR3-decorated RBCs were effectively capable of target cell killing in a model of pancreatic cancer. TR3 represents a generally applicable platform tool to study basic mechanisms along the death receptor pathway. More importantly, the ability to target TR3 to a cell surface presents the opportunity to create a cancer-selective drug with fewer off-target toxicities and enhanced killing capacities. *Mol Cancer Ther*; 9(7); 2142–51. ©2010 AACR.

## Introduction

When a cell is instructed to die in a coordinated fashion, it is considered to undergo apoptosis, or programmed cell death (1). Apoptosis is an important mechanism during early development but is also vital to maintain homeostasis of the immune system throughout life (2). Apoptosis is induced by two mechanisms, namely, the extrinsic or death receptor pathway and the intrinsic or the mitochondrial pathway (3–6). The extrinsic death pathway is triggered by ligand-receptor interactions that lead to intracellular signaling events, which ultimately result in the death of the target cell. One such ligand is represented by a member of the tumor necrosis factor (TNF) super-

family, TNF-related apoptosis-inducing ligand (TRAIL or Apo2L; refs. 7, 8). TRAIL interacts with at least five endogenous receptors, four of which are cell membrane associated [TRAIL-R1/death receptor 4 (DR4), TRAIL-R2/DR5, TRAIL-R3/decoy receptor 1 (DcR1), and TRAIL-R4/DcR2], whereas the fifth receptor, osteoprotegerin, constitutes a fluid-phase protein found in the circulation (9), with the potential to support tumor growth by blocking TRAIL binding to its activating cell surface receptors (10). Although TRAIL binds to all of these receptors, only ligation with DR4 and DR5 has been shown to induce apoptosis. Importantly, TRAIL-based therapeutics have been shown to be more effective inducers of apoptosis in cancer cells than in normal cells (11, 12). The mechanism underlying this tumor selectivity, however, is not fully elucidated. The intrinsic cancer selectivity represents one of the main reasons for the attractiveness of this molecule as an anticancer drug (13).

Endogenous TRAIL exists as a homotrimer, a critical requirement for its biological function. Various expression systems have been explored, and much progress has been made to obtain biologically active TRAIL proteins such as nontagged and tagged (FLAG, His, etc., with or without tag-mediated crosslinking), inclusion of trimerization domains such as a leucine zipper and/or an isoleucine zipper, and stabilization of the trimers with cations (i.e., zinc; ref. 14). In all previous reports, the

**Authors' Affiliations:** Departments of <sup>1</sup>Surgery and <sup>2</sup>Anesthesiology, Washington University School of Medicine, and Siteman Cancer Center, St. Louis, Missouri

**Note:** Supplementary material for this article is available at Molecular Cancer Therapeutics Online (<http://mct.aacrjournals.org/>).

**Corresponding Authors:** William G. Hawkins, Department of Surgery, Washington University School of Medicine, 660 S. Euclid Avenue, Campus Box 8109, St. Louis, MO 63110. Phone: 314-362-7046; Fax: 314-747-2977. E-mail: [hawkinsw@wustl.edu](mailto:hawkinsw@wustl.edu) or Dirk Spitzer, Department of Surgery, Washington University School of Medicine, 660 S. Euclid Avenue, Campus Box 8109, St. Louis, MO 63110. E-mail: [spitzerdm@hotmail.com](mailto:spitzerdm@hotmail.com)

doi: 10.1158/1535-7163.MCT-10-0225

©2010 American Association for Cancer Research.

building block for trimeric, recombinant TRAIL has been expressed from monomer-encoding cDNA sequences and has required self-association into functionally active trimers.

Capitalizing on the inherent antitumor properties of TRAIL, we have developed and tested a novel TRAIL expression construct, designated TR3. Additional modifications showed its potential as an investigative tool and as a platform on which to build cell-targeted anticancer therapeutics.

## Materials and Methods

### Proteins and antibodies

Recombinant human TRAIL (aa 114-281) was purchased from Enzo Life Sciences (formerly BIOMOL International). Antihuman TRAIL polyclonal antibody (rabbit) was obtained from Peprotech. FITC-conjugated antihuman IgG was purchased from Sigma, the Annexin-V/FITC apoptosis kit was purchased from Biosource, and cell viability was determined using a luciferase-based readout (CellTiter-Glo, Promega).

### Construction of expression plasmids

The wild-type, NH<sub>2</sub>-terminal ectodomain of human TRAIL (TR) described in this study contains amino acids 91 to 281 (domain I; compare Fig. 1A, including the striped box; the white box represents aa 114-281 of rTRAIL). A 594 bp DNA fragment amplified by PCR from a human U937 cDNA library (15) was inserted via *Bsi*WI (5') and *Hind*III (3') into sT-DAF (16). This basic TRAIL plasmid, designated pTRBg1, contains an additional *Bgl*II site immediately upstream of TRAIL's native stop codon for subsequent cloning purposes. It also contains a signal peptide to ensure secretion of the protein.

Following linearization of pTRBg1 with *Bgl*II and *Hind*III, the slightly smaller PCR-derived domains I' (5' *Bam*HI and 3' *Hind*III), containing amino acids 108 to 281 of native TRAIL, were added stepwise resulting in pTR2 (intermediate) and pTR3, respectively. The NH<sub>2</sub>-terminal enhanced green fluorescent protein (eGFP) extension of TR3 was introduced as an *Eco*RI/*Bsi*WI PCR fragment into pTR3, resulting in the eGFP-TR3 fusion protein (Supplementary Fig. S1A). Similarly, scFv-TR3 was generated by inserting the 735 bp *Bsi*WI scFv Ter-119 fragment from sT-DAF into the *Bsi*WI-linearized pTR3 plasmid. The chimera comprising the complement regulatory proteins DAF [short consensus repeat 1 (SCR1)] and CR1 (SCRs 15-17), targeted to the mouse RBC membrane via scFv Ter-119, has been described earlier (Ter-CR1, D.S. and J.P. Atkinson, unpublished data). This cDNA served as a PCR template to generate a scFv-DAF-CR1 fragment that was flanked by the restriction sites *Xho*I (5') and *Sna*BI (3'). This first fragment was then combined with a *Sna*BI/*Hind*III PCR-derived TR3 fragment and the *Xho*I/*Hind*III backbone of pSBC-1 (17), resulting in the spacer-containing scFv-S-TR3 form (Supplementary Fig. S1A). All PCR-derived DNA fragments were verified by DNA sequencing (Washington University Sequencing Core).

### Cells, transfections, and protein production

Human embryonic kidney cells [HEK293T, American Type Culture Collection (ATCC), CRL-11268] were used for protein generation. They were maintained in DMEM (Invitrogen) containing 10% FCS (Harlan). Media were supplemented with L-glutamine (Sigma), nonessential amino acids (BioWhittaker), and penicillin and streptomycin (Cellgro, Mediatech). The human T-cell line Jurkat (ATCC, TIB-152) and the pancreatic cancer cell line

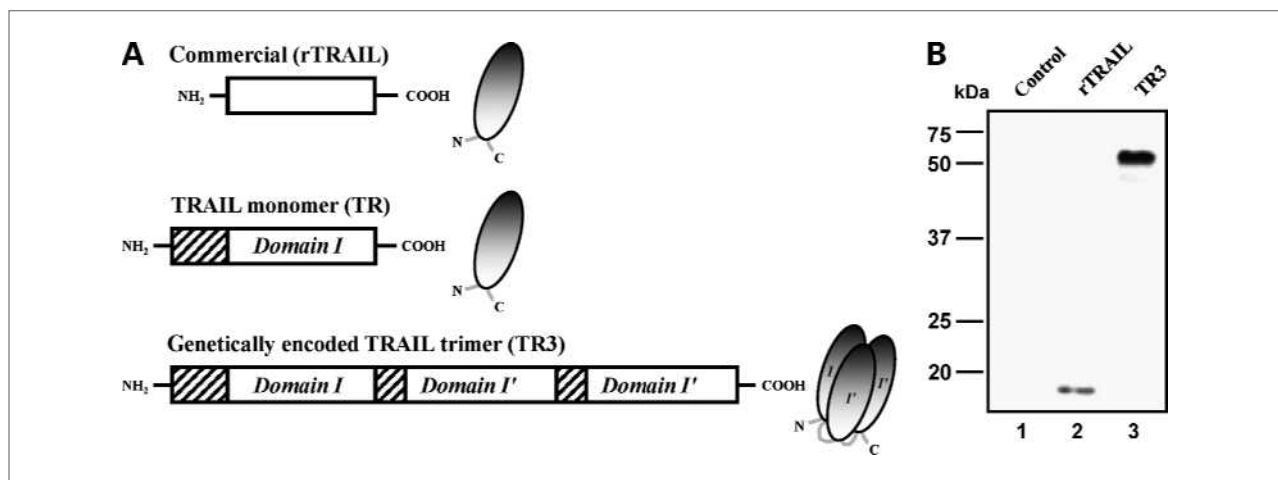


**Figure 1.** Design and biochemical characterization of the genetically encoded TRAIL trimer TR3. A, schematic representation of the TRAIL forms used in this study: commercially available TRAIL (rTRAIL, aa 114-281), domain I fragment (TR, aa 91-281), and the TR3 fusion protein. The bioactive domain of secreted TRAIL (TR) was joined three times to result in TR3. Striped boxes, native TRAIL sequence that is slightly smaller in domains I' (aa 108-113) compared with domain I (aa 91-113). B, Western blot analysis (reducing conditions) of commercially available rTRAIL (18 kDa, lane 2) and TR3 produced by HEK293T cells (~61 kDa, lane 3). Supernatant from mock-transfected HEK293T cells served as a negative control (lane 1).

BxPC3 (ATCC, CRL-1687) were maintained in RPMI1640 medium (Invitrogen), supplemented with 10% FCS, L-glutamine, and penicillin/streptomycin.

The recombinant TR3 forms and soluble death receptor 5 (DR5-Fc, kindly provided by Thomas Griffith, University of Iowa) were prepared by transient expression in HEK293T cells using Gibco Opti-Mem serum-free medium and TransIT-293 (Mirus, MIR2700) transfection reagent, as per the manufacturer's instructions. To obtain concentrated TR3 protein stocks, the supernatants were applied to centrifugal filter devices with a 10 kDa molecular cutoff (Centricon Plus-20, Millipore). DR5-Fc was purified using Protein A columns as per the manufacturer's instructions (Pierce). Protein concentration was determined with a spectrophotometer using bovine serum albumin (New England Biolabs) as a standard.

### Animals

C57BL/6 wild-type (WT) mice were used as an erythrocyte source and as recipients for recombinant TRAIL forms. Blood was collected from the tail vein using heparinized glass capillaries for coating experiments with scFv-(S)-TR3 and for the generation of plasma. Six- to eight-week-old male nude mice (*nu/nu*; Harlan) were used as hosts for tumor xenografts. Human BxPC3 tumor cells ( $5 \times 10^5$  cells/animal) were injected s.c. into the right flanks of the mice along with 40 times of mouse RBCs [ $2 \times 10^7$ , effector:target (E:T) ratio = 40] in a total volume of 50  $\mu$ L of FCS-free culture medium. The tumor size was measured with calipers using the following formula: Volume =  $0.5 (\text{length} \times \text{width}^2)$  (ref. 18). Procedures involving mice were approved by the Washington University Animal Studies Committee and conducted in accordance with the guidelines for the care and use of laboratory research animals established by the NIH.

### In vitro coating of mouse RBCs with targeted TR3

Several concentrations of mouse blood and TR3-containing culture supernatants were used as described in the text and figure legends. Briefly, 1 to 4  $\mu$ L of mouse whole blood ( $\sim 1\text{--}4 \times 10^7$  RBCs) were incubated with up to 1.5 mL of the filtered, HEK293T culture supernatant for 2 hours at room temperature, washed, and then processed for flow cytometry or subjected to coculture experiments with human Jurkat and BxPC3 cells. Supernatants from nontransfected HEK293T cells served as a control.

### Cell death determinations

The killing capacity of our novel TR3 forms was routinely assessed using a morphology-based fluorescence-activated cell scan (FACS) assay using Jurkat reporter cells. This procedure gave identical results compared with a standard Annexin-V/propidium iodide staining protocol (Supplementary Fig. S2). Unless otherwise stated, the simplified protocol was used to compare the cell killing activities of the various TRAIL forms.

A FACS-based viability assay was similarly used when RBCs were present during apoptosis measurements (Supplementary Fig. S3). Data acquisition was done on a FACScan flow cytometer (Becton & Dickinson). The data were analyzed with FlowJo software (Version 7.2.5, Tree Star). Cell viability of adherent cells was determined by crystal violet staining after fixation with 2% paraformaldehyde and CellTiter-Glo (Promega) according to the manufacturer's instructions. Data were recorded with a luminescence plate reader (Molecular Devices, SpectraMAX-Gemini, SoftMax Version 5 software).

### Statistical analyses

Linear regression analysis of RBC-mediated Jurkat and BxPC3 cell killing was calculated using Microsoft Excel software. Tumor growth curves are expressed as means  $\pm$  SE. A nonparametric, one-tailed *t*-test was done to evaluate the statistical significance of the two curves and individual data points using GraphPad Prism (V 4.02) software.

## Results

### Design and characterization of the genetically encoded human TRAIL trimer TR3

The recombinant, mature form of human TRAIL described here (TR3) comprises three consecutive extracellular TRAIL domains (with >99% TRAIL-specific amino acid sequence) fused together in a head-to-tail configuration (Fig. 1A). The single-chain character of the fusion protein was verified by Western blot analysis. Under reducing conditions, commercially available recombinant TRAIL (rTRAIL, aa 114-281) exhibits a molecular weight of 18 kDa, and TR3 has a molecular weight of  $\sim 61$  kDa, consistent with its calculated size (Fig. 1B).

To obtain evidence for its cell-killing activity, we treated TRAIL-sensitive human Jurkat cells with TR3 or rTRAIL. A FACS-based cell-killing assay was established that takes advantage of the morphologic changes (cell shrinkage) that are induced during apoptosis (Supplementary Fig. S2). We found that this new drug candidate revealed a strong apoptosis-inducing capacity (Fig. 2A, top), nearly identical to rTRAIL (Fig. 2A, bottom). To confirm that the killing activity was mediated by the death receptor pathway, we did a blocking experiment using DR5-Fc. DR5-Fc reduced the killing capacity of TR3 to background levels in a dose-dependent fashion (Fig. 2B, top), similar to that of rTRAIL (Fig. 2B, bottom, and Supplementary Fig. S4). The faster response of TR3 to DR5-Fc solely reflects the higher starting concentration of rTRAIL chosen for this particular experiment and requires a higher dose of soluble receptor to achieve rTRAIL blockade. In any case, this critical inhibition experiment suggests that TR3 assumes a native conformation, capable of interacting both with soluble DR5 and, more importantly, with cell-bound DR5 (the only death receptor expressed from

Jurkat T cells; data not shown), through which it stimulates the extrinsic death pathway and ultimately induces target cell death. Finally, to obtain additional evidence for the unaltered specificity profile of TR3, we treated nontransformed, immortalized human pancreatic ductal epithelial cells with TR3 and rTRAIL. We found that both reagents did not cause cell death on these normal cells, which is consistent with the notion that TRAIL preferentially kills transformed target cells (data not shown).

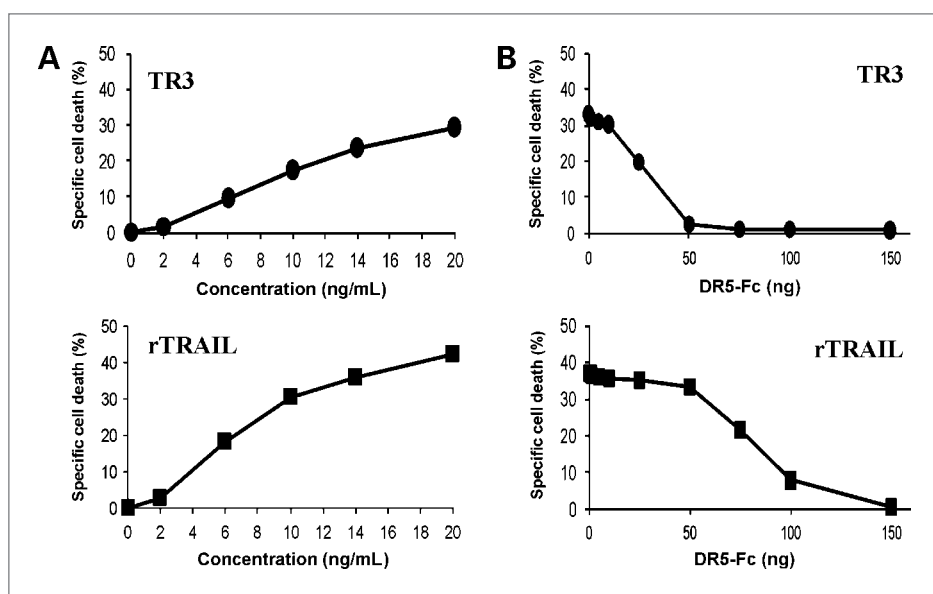
To assess the physicochemical properties of TR3 using defined *in vitro* conditions, we evaluated (a) its stability during storage at physiologic temperature and (b) the consequences of repeated freeze/thaw (F/T) cycles. When maintained at 37°C, commercially available rTRAIL readily lost a significant fraction of its initial killing potential (Fig. 3A; >95% reduction after 30 min). In contrast, TR3 was unaffected by this treatment and retained 100% of its activity following a 6-hour incubation period at 37°C (Fig. 3A). We also assessed the effect of repeated F/T cycles on the stability of TR3 compared with rTRAIL. We noted a rapid loss of activity of rTRAIL following only one F/T cycle ranging between 90% and 95% compared with the nonfrozen control (Fig. 3B). No residual killing activity was generally detected past the third F/T cycle. In contrast to rTRAIL, TR3 retained 100% of its biological activity even when cycled 10 times (Fig. 3B). Finally, when TR3 and rTRAIL were injected *i.v.* into WT C57BL/6 mice and plasma was collected and tested for biological activity at 1 minute (baseline) and 10 minutes postinjection, we found that rTRAIL lost a significant fraction of its activity within the first 10 minutes in circulation (Fig. 3C;  $49.0 \pm 8.4\%$  reduction), whereas TR3 maintained its bioactive form longer (Fig. 3D;  $13.8 \pm 1.5\%$  reduction). These results show that covalently linked TRAIL monomers (TR3) have more favorable

pharmacokinetic characteristics than noncovalently associated rTRAIL. The improved stability of TR3 over rTRAIL, especially *in vivo*, may prove to be a significant advance for researchers as well as clinicians.

### Genetically encoded domain additions do not interfere with TR3 function

Building on the improved pharmacologic stability of TR3, we addressed next how additional genetically encoded alterations (domain additions) would affect the performance of TR3. The goal of such an approach was to direct TRAIL activity more specifically to a predefined target to further increase its cell specificity and reduce its off-target effects following systemic application. Examples of an extremely functionally diverse but structurally homogeneous class of cell targeting devices are single-chain antibody fragments (scFv). Encoded by single genetic fusion sequences themselves, they are versatile entities that would allow TR3 to be targeted to a selected site and would therefore provide a secondary specificity besides the natural affinity of TRAIL for the death-inducing receptors. As a proof of concept, we introduced a scFv to the NH<sub>2</sub>-terminus of TR3 that recognizes glycoporphin A on the mouse RBC (scFv-TR3; Supplementary Fig. S1A). This model antigen was chosen because of the lack of endogenous TRAIL receptors on the RBC membrane, and it would better facilitate our ability to interpret the results of target cell binding studies (see below). In anticipation of potential steric constraints, we designed an additional RBC-targeted TR3 form to create a larger distance between the scFv and TR3 (scFv-S-TR3; Supplementary Fig. S1A). This elongated spacer comprised four SCRs, ~60 amino acid-containing globular domains of the human complement regulatory proteins decay accelerating factor (DAF, CD55) and complement receptor 1 (CR1, CD35). To show the broad

**Figure 2.** TR3 is a powerful inducer of apoptosis. A, a FACS-based apoptosis assay (see also Supplementary Fig. S1) with human Jurkat cells shows the dose-dependent killing capacity of TR3 in comparison with rTRAIL. Protein concentration of TR3 was determined by semiquantitative Western blot analysis using known amounts of purchased rTRAIL as a reference. B, dose-dependent blocking of TR3 activity with soluble death receptor 5 (DR5-Fc) assayed on Jurkat cells as described above for A. Representative dose-response curves from four replicate experiments are shown.



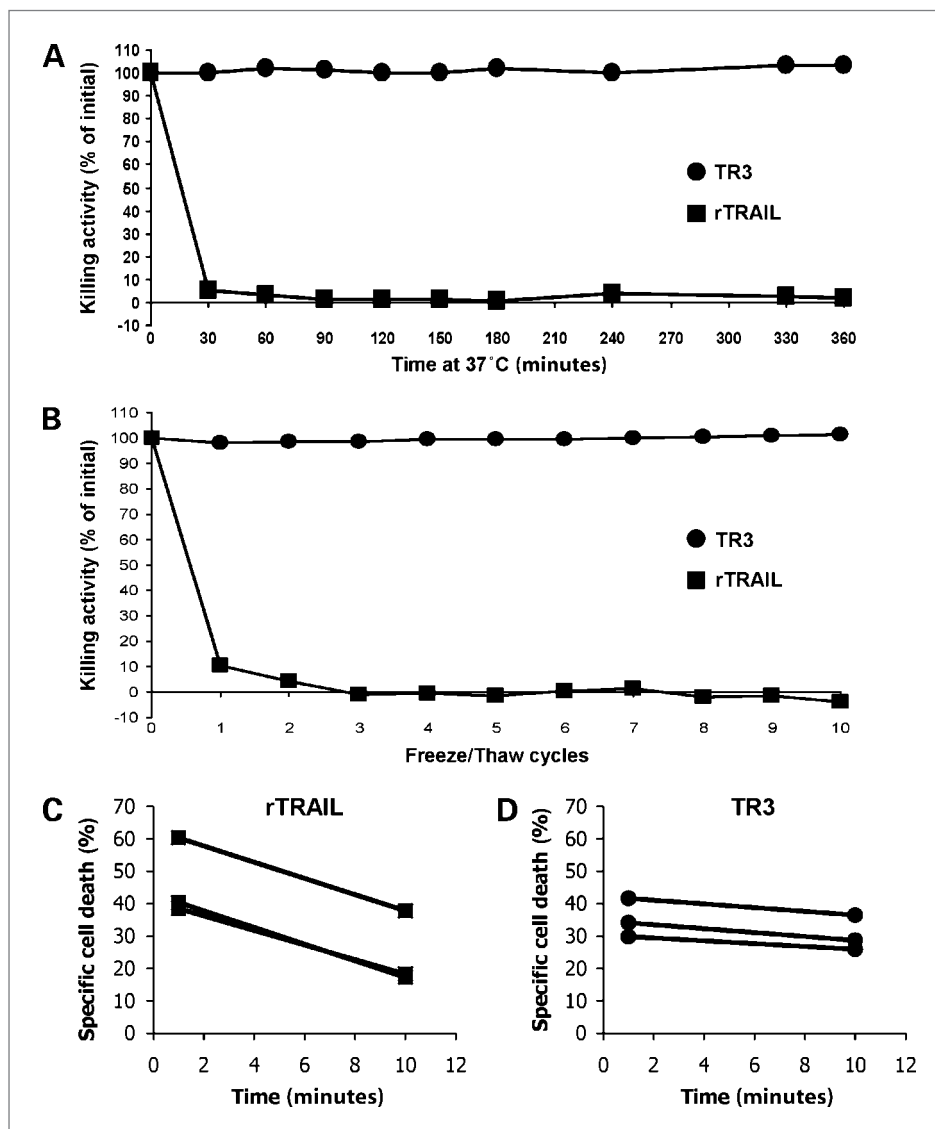


**Figure 3.** TR3 has improved pharmacologic characteristics *in vitro* and *in vivo*. A, TR3 and rTRAIL were kept at 37°C for the indicated times. Samples were obtained and kept on ice until used in a FACS-based killing assay described for Fig. 2. B, the same killing assay as in A, but the reagents were subjected to up to 10 freeze/thaw cycles. Representative killing curves from three replicate experiments are shown. rTRAIL (C) and TR3 (D) were injected i.v. into the tail vein of WT C57BL/6 mice and plasma was collected at the indicated time points. Death-inducing activity was then determined using Jurkat target cells as described for A and B. Of note, the activity loss of each compound was nearly identical for each mouse (similar slope) but differed markedly between the two compounds (steeper slope for rTRAIL than for TR3).

applicability of our platform technology, we also added eGFP as another fusion partner of TR3 (eGFP-TR3; Supplementary Fig. S1A).

All fusion constructs were expressed in HEK293T cells and exhibited their expected molecular weights determined by Western blot analysis (scFv-TR3 at 85 kDa, scFv-S-TR3 at 110 kDa, and the eGFP-tagged TR3 at 85 kDa; Supplementary Fig. S1B). To evaluate the impact of the NH<sub>2</sub>-terminal extensions of each fusion protein, the fluid-phase killing capacity of the additional TR3 variants was tested and compared with the parental molecule. Interestingly, we found that all TR3 forms were capable of inducing apoptosis on DR5-expressing Jurkat reporter cells (Supplementary Fig. S1C). This result was encouraging from the perspective of designing future therapeutic drugs because we found that attachment of a 50 kDa heterologous,

non-TRAIL sequence (scFv-S-TR3) did not sterically hinder the killing capacity of TR3.

#### Target cell killing with TR3-decorated RBCs *in vitro*

Although the ultimate objective was to target TR3 directly to a tumor cell membrane, we believed it was necessary to ask if scFv-TR3, and its spacer variant scFv-S-TR3, could be selectively attached to a cell membrane that lacks a TR3 binding partner. Again, the RBC was chosen because it represents a death receptor-deficient cell type. The respective TRAIL forms were incubated with C57BL/6 mouse whole blood, washed, and assessed for the presence of TR3 on the RBC membranes using purified DR5-Fc. Indeed, FACS analysis revealed a strong, homogeneous signal peak for both RBC-targeted TR3 variants (Fig. 4A). In addition, scFv-S-TR3 was also detected with an antihuman CR1 monoclonal antibody (clone 3D9),

which binds to the spacer region of the fusion protein (Supplementary Fig. S1D and E). The fact that a soluble DR5 receptor was capable of binding RBC-bound TR3 suggests that the death receptor-interacting domains of these large fusion proteins were folded correctly and should be also accessible by membrane-expressed DR5 on a given target cell. To prove this hypothesis, we used a rosetting assay, in which TR3-coated murine RBCs (compare Fig. 4A for coating levels) were mixed with eYFP-expressing Jurkat target cells and were allowed to sediment at ambient temperature. We anticipated that the fusion proteins would facilitate bridging of the two cell types and consequently form aggregates (rosettes). Shortly after mixing, we identified mouse RBCs (red) tightly attached to their green target cells (Fig. 4B, arrows). Importantly, this was true only for the spacer version of TR3 (scFv-S-TR3), because we did not observe a rosetting phenomenon in the absence of the spacer (scFv-TR3; data not shown). Moreover, once the RBCs attached to their targets, we observed programmed cell death as documented by the appearance of apoptotic bodies (Fig. 4B, arrowhead).

We next sought to quantitatively investigate the RBC-mediated target cell killing and study the impact of the spacer domain of scFv-S-TR3 with respect to TRAIL receptor recognition once immobilized to the RBC surface. The relative copy numbers of the RBC-bound TR3 forms were determined by DR5-Fc staining (compare Fig. 4A for TR3 coating levels). We specifically chose to attach more copies of the spacer-deficient scFv-TR3 to the RBCs because we had already shown that only the spacer variant was capable of forming rosettes, suggesting that it would likely be a more powerful inducer of target cell apoptosis. A FACS-based Jurkat killing assay in the presence of RBCs was used similar to what has been described above (Supplementary Fig. S3). As anticipated, the presence of medium-treated control RBCs had no effect

on the viability of the target cells (Fig. 5A). In contrast, we found that both RBC-targeted TR3 forms elicited cell death in this coculture system (Fig. 5A). In this comparative killing assay using only limited TR3 copy numbers attached to the RBC surface (<5,000 estimated copies/RBC), the spacer variant scFv-S-TR3 was more than twice as effective as the nonspacer form scFv-TR3 (based on the slopes of the killing curves) although we provided a much reduced copy number of the spacer variant attached to the RBC membrane (only 60% relative to scFv-TR3). It is worth mentioning that it was only possible to do these binding and killing experiments because of the improved stability of the TR3 molecule, since the coating process was done for several hours at ambient temperature, conditions under which rTRAIL would have lost its bioactivity.

To rule out that the RBC-mediated target cell killing was not induced by contaminating fluid-phase fusion proteins, we carried out a similar experiment but spatially separated effector and target cells using a transwell system. Under these conditions, target cell killing was completely abolished, confirming that TR3-decorated RBCs induce apoptosis via cell-cell contact (data not shown).

In the experiments described above, we coated the RBCs prior to coculture with their Jurkat target cells. In this setting it was difficult to compare the results with regard to the exact number of TR3 molecules bound to the RBC membrane with nonbound, fluid-phase TR3. To address this issue, increasing numbers of naïve RBCs were added first to the target cells. Then, functionally equivalent doses of RBC-targeted scFv-S-TR3 and, as a control, nontargeted TR3 (with identical fluid-phase killing activities), were added to the mixtures. As expected, in the presence of non-RBC-targeted TR3, increasing numbers of RBCs did not improve (or reduce) target cell killing (Fig. 5B, killing

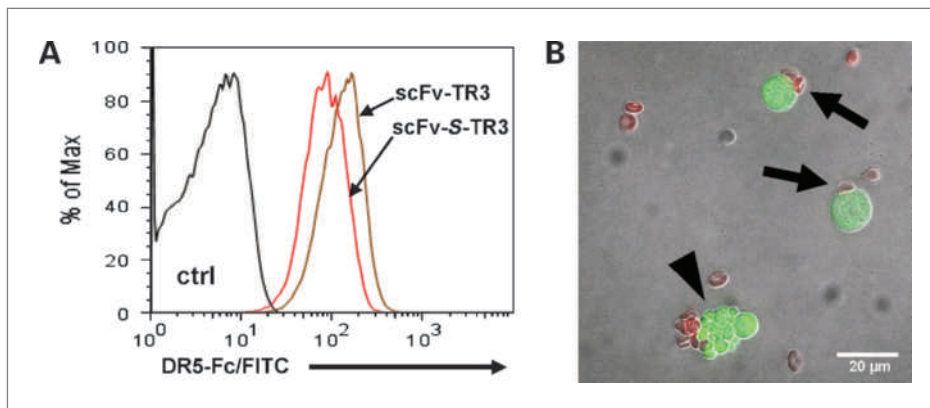


**Figure 4.** TR3-coated RBCs attach to death receptor–positive target cells. **A**, RBC binding of NH<sub>2</sub>-terminally extended TR3 variants was verified by FACS analysis using DR5-Fc, detected with FITC-conjugated antihuman IgG. **B**, mouse RBCs were labeled with the red membrane dye PKH-26 (Sigma) and then coated with scFv-S-TR3. They were then mixed and allowed to sediment with eYFP-expressing Jurkat cells at ambient temperature for 1 hour. Sequential images were taken with an epifluorescent microscope and then merged. This representative image shows tight binding between RBCs and Jurkat cells (arrows) and formation of apoptotic structures of the target cells (arrowhead). Original magnification,  $\times 20$ .

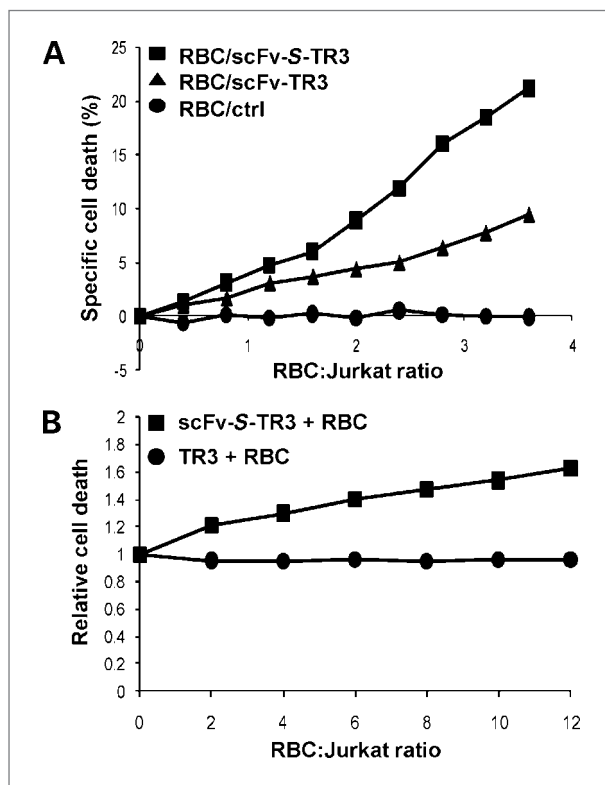


**Figure 5.** RBC-targeted TR3 kills tumor cells *in vitro*. A, naïve and TR3-coated mouse RBCs (compare Fig. 4A for the respective coating levels) were cocultured at different ratios with Jurkat target cells for 24 hours and subsequently analyzed for cell viability (Supplementary Fig. S4). The killing capacity of the spacer form scFv-S-TR3 was more than twice as potent (2.45-fold), although its copy number was only ~60% that of scFv-TR3 (linear regression analysis,  $R^2 = 0.973$  for scFv-S-TR3, and  $R^2 = 0.98$  for scFv-TR3). Representative killing curves from three replicate experiments are shown. B, a similar experiment as described in A, but this time naïve RBCs were mixed first with their Jurkat target cells at increasing ratios. Then, a constant amount of RBC-targeted or nontargeted TR3 (control) was added to the wells and analyzed for apoptosis induction 24 hours later (baseline apoptosis 50% for both reagents in the absence of RBCs). Representative killing curves from two replicate experiments are shown.

curve remains horizontal). However, increasing concentrations of naïve RBCs during the treatment period with scFv-S-TR3 resulted in an increased target cell killing of >60% at the highest RBC concentration used, likely via *in situ* RBC coating (Fig. 5B). Interestingly, although the drug input was the same under these different conditions (baseline, fluid-phase killing for both drugs in the absence of RBCs ~50%), enhanced target cell killing was only possible in the presence of a “native” solid matrix, i.e., the RBC membrane. Experiments are currently planned to investigate the nature of the enhanced killing capacity of surface-immobilized TR3 in greater detail. Together, these results suggest that it should be feasible to decorate, via single-chain antibody fragments, a tumor cell surface with biologically active TR3 potentially augmenting the native killing capacity of TRAIL while decreasing systemic toxicity.

### Target cell killing with TR3-decorated RBCs reduces tumor growth

To assess the ability of RBC-targeted TR3 to kill human tumor cells, we used a murine xenotransplantation model of pancreatic cancer. We first confirmed the previously reported TRAIL sensitivity of BxPC3 cells by cocultivation with TR3-decorated mouse RBCs in a similar tissue culture system described above for the Jurkat T-cell line. We found that BxPC3 cells were killed by TR3-coated RBCs in a dose-dependent fashion (Fig. 6A).

To assess the killing capacity of TR3-decorated RBCs, we had to ensure that effector and target cells would have access to each other. Therefore, BxPC3 cells were mixed on ice (to prevent immediate rosette formation) with scFv-S-TR3-coated mouse effector RBCs at an E:T of 40 (with  $5 \times 10^5$  target cells/animal) and immediately injected into the right flanks of male nude mice. It was expected that in this particular model, at an E:T of 40, a similar fraction of the tumor targets would be eliminated (~60%; Fig. 6B, inset) within the first 24 hours after implantation due to direct and required cell contact with TR3-coated RBCs. We expected that the surviving cells (~40%) would engraft and eventually contribute to tumor formation. This is indeed what we observed. Eight days postinoculation, the control animals developed measurable tumor masses that continued to grow exponentially (Fig. 6B). In contrast, mice that received a mixture of BxPC3 and TR3-coated RBC effector cells presented with a ~30-day delay in tumor progression, after which the growth characteristics were identical to the tumors in the control animals.

### Discussion

TRAIL is a member of the TNF superfamily and is well known for its ability to cause cancer-selective apoptosis. A number of different approaches have been utilized in the past to produce biologically active TRAIL trimers, and are all based on the expression of monomeric cDNAs. In this study, recombinant human TRAIL trimers (TR3 family) were generated based on a single polypeptide format. We showed the potent apoptosis-inducing activity of TR3, similar to rTRAIL but with an enhanced stability profile compared with the latter. We further believe that the genetic approach to trimerization will extend to other TNF family members. In fact, we found that a similar concept has been reported for TNF, and similar to TR3, recombinant TNF trimers also showed increased stability compared with their noncovalently associated form (19). However, the most important finding of our current work is the fact that TR3 can be further genetically modified while TRAIL activity remains fully preserved.

In this report, we show the feasibility of such modifications by incorporating cell-targeting epitopes to the parental TR3 molecule. As an example, we have shown that an antibody fragment (scFv) with specificity for

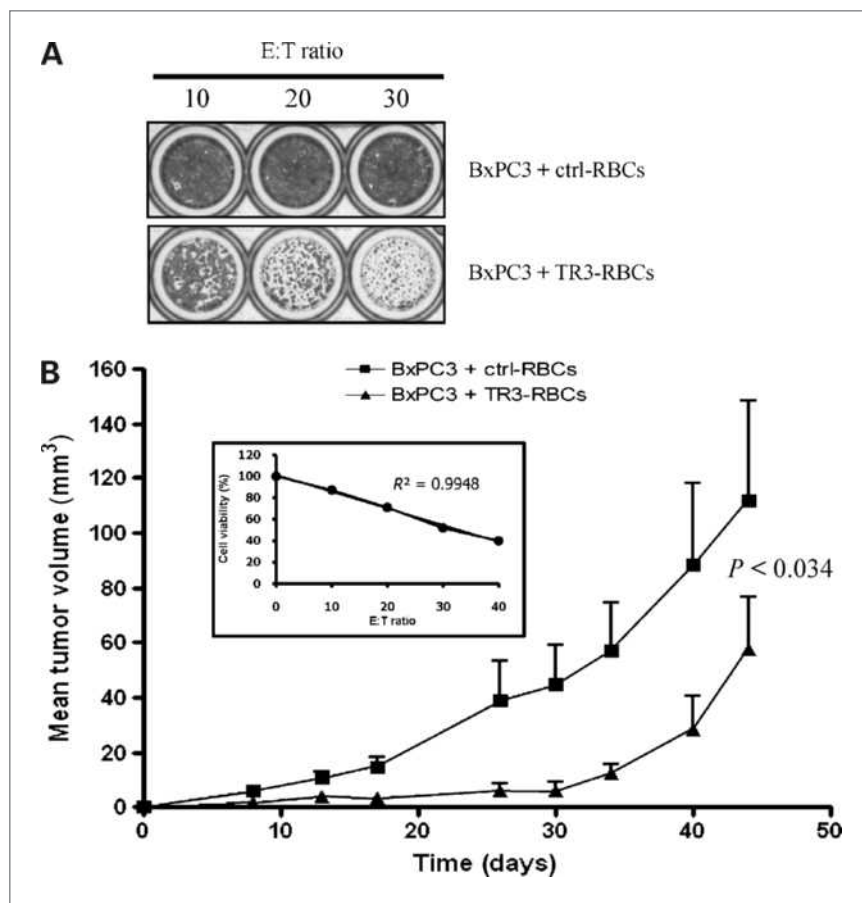
mouse RBCs to the NH<sub>2</sub>-terminus of TR3 allowed us to deliver bioactive TRAIL to a native cell membrane in a stoichiometrically controlled fashion. This latter point represents another key feature of the TR3 platform technology and means that one targeting molecule (scFv) could deliver a prearranged, bioactive TRAIL trimer (TR3) to a defined target site. Therefore, changing the scFv fragment to one that specifically targets a cancer cell may reduce some of the off-target toxicity associated with other rTRAIL formulations (9). A similar strategy has been recently applied using a monomeric TRAIL-encoding scFv fusion construct (20–22), which generated predominantly monomeric as well as dimeric and only a minor fraction of biologically active trimeric complexes (22). Therefore, we believe that the steric control provided by our assembly strategy (scFv:TR3 = 1:3) would significantly expand on the size and nature of attachments to TR3 than we would envision to encounter by combining three TRAIL molecules, each carrying a cell targeting antibody fragment.

Another important modification we explored was the elongated spacer domain, inserted between the targeting scFv and TR3. This configuration was expected (a) to better enable binding to the RBC via scFv and (b) to elevate the TR3 domain farther away from the RBC surface,

thereby better allowing an interaction with target cell-expressed death receptors. Although we do not present evidence for the spacer being advantageous for optimal target cell binding, we found that, when RBC bound, this spacer substantially enhanced the activity of the drug compared with its spacer-deficient analog. The fact that such a spacer-containing TR3 molecule was capable of bridging two unrelated cell types (TR3-decorated RBCs and Jurkat/BxPC3 cells) and could induce apoptosis via cell-cell contact, suggests that a future anticancer therapeutic based on this design should be as capable of bridging tumor-specific antigens and DR4/5 located on the same cell (*cis*-effect) as well as adjacent cells (*trans*-effect) causing apoptosis of both tumor cells.

Finally, the nearly complete absence of artificial linker sequences of TR3 and the incorporation of spacer sequences with human origin, human DAF and CR1 domains (scFv-S-TR3), has the theoretical advantage of reducing potential immunogenicity of a novel therapeutic based on this technology. However, this aspect and immunogenicity due to generation of neoepitopes need to be evaluated in a small animal model, i.e., using mouse TRAIL for the construction of murine TR3 and the respective murine-derived spacer sequences.

**Figure 6.** Human pancreatic cancer cells were killed *in vivo* following coinjection with TR3-coated RBCs. **A**, *in vitro* killing of the pancreatic cancer cell line BxPC3 with TR3-RBCs. A similar experiment as described for Fig. 5A in which the Jurkat cells were replaced with BxPC3 cells. Following a nonenzymatic cell detachment procedure (PBS/EDTA), the target cells were mixed at the indicated E:T ratios with naïve and scFv-S-TR3-coated mouse RBCs. The mixtures were then cocultured for 24 hours, and the cell viability was determined after fixation with 2% paraformaldehyde using crystal violet. **B**, BxPC3 cells were mixed with TR3-coated RBCs (scFv-S-TR3) at an E:T ratio of 40 immediately prior to s.c. injection into the flanks of nude mice. Medium-treated RBCs served as controls. A luminescent cell viability assay was used in parallel to verify the killing capacity of the RBC-preparation (inset). Tumor size was monitored by caliper measurements at the indicated time points and is expressed as means  $\pm$  SE. Each group,  $n = 5$ ;  $P < 0.034$  (unpaired *t*-test).



Secreted TRAIL, expressed from a monomeric cDNA in mammalian cells, is mostly inactive (23). This has been attributed mainly to the formation of interchain disulfide bridges, which in turn causes this mixture of TRAIL monomers, dimers, and trimers to have reduced affinity for its cell surface receptors. We have been able to confirm these results and only the enforced trimer formation via an isoleucine-zipper domain could restore TRAIL activity (data not shown). Therefore, trimer enforcement via generation of TR3 resembles more closely an isoleucine zipper-TRAIL configuration in that formation of these disulfide bridges is likely being disabled because TR3 is biologically highly active when produced from mammalian cells. These findings have important consequences if biochemical postproduction manipulations are not an option. One example represents gene therapy in which the patient's own (mammalian) cells are the source of the therapeutic protein. Although such a concept has been investigated (24), it seems likely that TR3 could represent a more powerful alternative over TRAIL produced from a monomer-encoding cDNA.

A potential activity-enhancing modification relates to the location where the additional fusion partners of TR3 were attached. We initiated our studies by fusing these domains to the NH<sub>2</sub>-terminus of TR3. However, we have recently shown that switching the scFv from the NH<sub>2</sub>- to the COOH-terminus of an RBC-targeted mouse complement regulator resulted in a substantial improvement of its activity (25). Theoretically, those types of variations could also improve the properties of tumor-targeted TR3 variants, considering that both termini of the TR3 fusion protein should be accessible in light of several reported crystallographic studies on non-covalently associated TRAIL trimers (26–29). Furthermore, TRAIL binding specificity can be tailored by genetic engineering (by introducing several amino acid substitutions) toward either of the two death-inducing receptors DR4 or DR5 (30), depending on which death receptor would represent the more promising therapeutic target. These types of alterations could be easily applied to TR3.

One unexpected observation requires further exploration. The addition of nontargeted TRAIL forms (TR3 and rTRAIL) to the Jurkat target cells consistently resulted in a plateau in killing at ~40% to 60%. This plateau effect has been considered a limitation of TRAIL-based

monotherapies (31). With TRAIL immobilized on a solid matrix (the RBC surface), this plateau was consistently overcome. Our initial observations indicate that there may be cell signaling advantages to a surface-based TR3 delivery platform which warrant further investigation.

In summary, we present a new method to generate recombinant human TRAIL (TR3-family) based on a single polypeptide format featuring potent apoptosis-inducing activity and enhanced stability. Importantly, TR3 can be further modified in a stoichiometrically controlled fashion without interfering with TRAIL function. To achieve higher target cell specificity and/or killing activity, we are currently adopting this platform to a variety of different tumor-associated antigens. This approach will take advantage of two ligand-receptor interactions facilitated by a single, multifunctional drug-tumor Ag:scFv and TR3:death receptor. As a consequence, we predict that the resulting multidomain therapeutic would have greater affinity for the tumor and a reduced affinity toward normal host cells. The predicted advantages of such a concept would be a stronger and more sustained induction of the death receptor pathway in the targeted tumor cells. As TRAIL has been shown to augment the effects of standard therapies, a tumor-targeted TR3 might further enhance the effectiveness of other chemotherapies while limiting off-target toxicities to the patients.

#### Disclosure of Potential Conflicts of Interest

No potential conflicts of interest were disclosed.

#### Acknowledgments

We thank Dr. Tom Ferguson for helpful comments, Dr. Thomas Griffith for providing the DR5-Fc expression plasmid, Jesse Gibbs for technical assistance, and Kim Trinkaus and Jingqin "Rosy" Luo (Washington University Biostatistician Core) for statistical advice.

#### Grant Support

NIH grants 5P30CA9184208 and 1R21CA150945 to D. Spitzer and W.G. Hawkins.

The costs of publication of this article were defrayed in part by the payment of page charges. This article must therefore be hereby marked *advertisement* in accordance with 18 U.S.C. Section 1734 solely to indicate this fact.

Received 03/05/2010; revised 04/20/2010; accepted 05/06/2010; published OnlineFirst 06/22/2010.

#### References

- Kerr JF, Wyllie AH, Currie AR. Apoptosis: a basic biological phenomenon with wide-ranging implications in tissue kinetics. *Br J Cancer* 1972;26:239–57.
- Vaux DL, Korsmeyer SJ. Cell death in development. *Cell* 1999;96:245–54.
- Ashkenazi A. Targeting death and decoy receptors of the tumour-necrosis factor superfamily. *Nat Rev Cancer* 2002;2:420–30.
- Fesik SW. Promoting apoptosis as a strategy for cancer drug discovery. *Nat Rev Cancer* 2005;5:876–85.
- Ghobrial IM, Witzig TE, Adjei AA. Targeting apoptosis pathways in cancer therapy. *CA Cancer J Clin* 2005;55:178–94.
- de Vries EG, Gietema JA, de Jong S. Tumor necrosis factor-related apoptosis-inducing ligand pathway and its therapeutic implications. *Clin Cancer Res* 2006;12:2390–3.
- Wiley SR, Schooley K, Smolak PJ, et al. Identification and characterization of a new member of the TNF family that induces apoptosis. *Immunity* 1995;3:673–82.
- Pitti RM, Marsters SA, Ruppert S, Donahue CJ, Moore A, Ashkenazi A. Induction of apoptosis by Apo-2 ligand, a new member of the

- tumor necrosis factor cytokine family. *J Biol Chem* 1996;271:12687–90.
9. LeBlanc HN, Ashkenazi A. Apo2L/TRAIL and its death and decoy receptors. *Cell Death Differ* 2003;10:66–75.
  10. Zauli G, Melloni E, Capitani S, Secchiero P. Role of full-length osteoprotegerin in tumor cell biology. *Cell Mol Life Sci* 2009;66:841–51.
  11. Falschlehner C, Emmerich CH, Gerlach B, Walczak H. TRAIL signaling: decisions between life and death. *Int J Biochem Cell Biol* 2007;39:1462–75.
  12. Walczak H, Miller RE, Ariail K, et al. Tumoricidal activity of tumor necrosis factor-related apoptosis-inducing ligand *in vivo*. *Nat Med* 1999;5:157–63.
  13. Garber K. New apoptosis drugs face critical test. *Nat Biotechnol* 2005;23:409–11.
  14. Merino D, Lalaoui N, Morizot A, Solary E, Micheau O. TRAIL in cancer therapy: present and future challenges. *Expert Opin Ther Targets* 2007;11:1299–314.
  15. Spitzer D, Mitchell LM, Atkinson JP, Hourcade DE. Properdin can initiate complement activation by binding specific target surfaces and providing a platform for *de novo* convertase assembly. *J Immunol* 2007;179:2600–8.
  16. Spitzer D, Unsinger J, Bessler M, Atkinson JP. ScFv-mediated *in vivo* targeting of DAF to erythrocytes inhibits lysis by complement. *Mol Immunol* 2004;40:911–9.
  17. Dirks W, Schaper F, Kirchhoff S, Morelle C, Hauser H. A multifunctional vector family for gene expression in mammalian cells. *Gene* 1994;149:387–8.
  18. Euhus DM, Hudd C, LaRegina MC, Johnson FE. Tumor measurement in the nude mouse. *J Surg Oncol* 1986;31:229–34.
  19. Krippner-Heidenreich A, Grunwald I, Zimmermann G, et al. Single-chain TNF, a TNF derivative with enhanced stability and antitumor activity. *J Immunol* 2008;180:8176–83.
  20. Ten CB, Bremer E, de Bruyn M, et al. A novel AML-selective TRAIL fusion protein that is superior to Gemtuzumab Ozogamicin in terms of *in vitro* selectivity, activity and stability. *Leukemia* 2009;23:1389–97.
  21. Bremer E, de Bruyn M, Samplonius DF, et al. Targeted delivery of a designed sTRAIL mutant results in superior apoptotic activity towards EGFR-positive tumor cells. *J Mol Med* 2008;86:909–24.
  22. Bremer E, Kuijlen J, Samplonius D, Walczak H, de LL, Helfrich W. Target cell-restricted and -enhanced apoptosis induction by a scFv:sTRAIL fusion protein with specificity for the pancreatic carcinoma-associated antigen EGP2. *Int J Cancer* 2004;109:281–90.
  23. Bodmer JL, Meier P, Tschopp J, Schneider P. Cysteine 230 is essential for the structure and activity of the cytotoxic ligand TRAIL. *J Biol Chem* 2000;275:20632–7.
  24. Griffith TS, Stokes B, Kucaba TA, et al. TRAIL gene therapy: from preclinical development to clinical application. *Curr Gene Ther* 2009;9:9–19.
  25. Spitzer D, Unsinger J, Mao D, Wu X, Molina H, Atkinson JP. *In vivo* correction of complement regulatory protein deficiency with an inhibitor targeting the red blood cell membrane. *J Immunol* 2005;175:7763–70.
  26. Mongkolsapaya J, Grimes JM, Chen N, et al. Structure of the TRAIL-DR5 complex reveals mechanisms conferring specificity in apoptotic initiation. *Nat Struct Biol* 1999;6:1048–53.
  27. Hymowitz SG, Christinger HW, Fuh G, et al. Triggering cell death: the crystal structure of Apo2L/TRAIL in a complex with death receptor 5. *Mol Cell* 1999;4:563–71.
  28. Cha SS, Kim MS, Choi YH, et al. 2.8 Å resolution crystal structure of human TRAIL, a cytokine with selective antitumor activity. *Immunity* 1999;11:253–61.
  29. Cha SS, Sung BJ, Kim YA, et al. Crystal structure of TRAIL-DR5 complex identifies a critical role of the unique frame insertion in conferring recognition specificity. *J Biol Chem* 2000;275:31171–7.
  30. Kelley RF, Totpal K, Lindstrom SH, et al. Receptor-selective mutants of apoptosis-inducing ligand 2/tumor necrosis factor-related apoptosis-inducing ligand reveal a greater contribution of death receptor (DR) 5 than DR4 to apoptosis signaling. *J Biol Chem* 2005;280:2205–12.
  31. Spencer SL, Gaudet S, Albeck JG, Burke JM, Sorger PK. Non-genetic origins of cell-to-cell variability in TRAIL-induced apoptosis. *Nature* 2009;459:428–32.

# Molecular Cancer Therapeutics

## A Genetically Encoded Multifunctional TRAIL Trimer Facilitates Cell-Specific Targeting and Tumor Cell Killing

Dirk Spitzer, Jonathan E. McDunn, Stacey Plambeck-Suess, et al.

*Mol Cancer Ther* 2010;9:2142-2151. Published OnlineFirst June 22, 2010.

<b>Updated version</b>	Access the most recent version of this article at: doi: <a href="https://doi.org/10.1158/1535-7163.MCT-10-0225">10.1158/1535-7163.MCT-10-0225</a>
<b>Supplementary Material</b>	Access the most recent supplemental material at: <a href="http://mct.aacrjournals.org/content/suppl/2010/06/22/1535-7163.MCT-10-0225.DC1">http://mct.aacrjournals.org/content/suppl/2010/06/22/1535-7163.MCT-10-0225.DC1</a>

<b>Cited articles</b>	This article cites 31 articles, 8 of which you can access for free at: <a href="http://mct.aacrjournals.org/content/9/7/2142.full#ref-list-1">http://mct.aacrjournals.org/content/9/7/2142.full#ref-list-1</a>
<b>Citing articles</b>	This article has been cited by 4 HighWire-hosted articles. Access the articles at: <a href="http://mct.aacrjournals.org/content/9/7/2142.full#related-urls">http://mct.aacrjournals.org/content/9/7/2142.full#related-urls</a>

<b>E-mail alerts</b>	<a href="#">Sign up to receive free email-alerts</a> related to this article or journal.
<b>Reprints and Subscriptions</b>	To order reprints of this article or to subscribe to the journal, contact the AACR Publications Department at <a href="mailto:pubs@aacr.org">pubs@aacr.org</a> .
<b>Permissions</b>	To request permission to re-use all or part of this article, use this link <a href="http://mct.aacrjournals.org/content/9/7/2142">http://mct.aacrjournals.org/content/9/7/2142</a> . Click on "Request Permissions" which will take you to the Copyright Clearance Center's (CCC) Rightslink site.